ELSEVIER

Journal of Power Sources 96 (2001) 204–213

JOURNAL OF POWER SOURCES

www.elsevier.com/locate/jpowsour

The effect of anode flow characteristics and temperature on the performance of a direct methanol fuel cell

John C. Amphlett, Brant A. Peppley*, Ela Halliop, Aamir Sadiq

Department of Chemistry and Chemical Engineering, Royal Military College of Canada, Kingston, Ont., Canada K7K 7B4

Received 6 December 2000; accepted 16 December 2000

Abstract

An experimental direct methanol fuel cell (DMFC), designed and manufactured in-house, was used in this study. The cell is of standard filter-press configuration with parallel rectangular single-pass anode channels. The membrane electrode assembly (MEA), with a suitable Pt–Ru anode electrocatalyst, was purchased from E-TEK Inc. A 1.0 M methanol in water solution was used as the fuel and pure oxygen was used as the oxidant in all experiments. Three graphite anode plates were machined with the same flow channel configuration but each with different depth of channels. The cathode was kept the same for all experiments. Polarisation curves and ac impedance spectra were obtained for varying temperatures and channel depths. To separate the contribution of the oxygen reduction reaction to the overvoltage from the anode and membrane contributions, reference hydrogen electrode (RHE) measurements were taken. By comparing the RHE polarisation with the methanol–oxygen polarisation experiments, it was found that polarisation losses at the oxygen cathode accounted for a 40–50% of the overpotential.

The variation in the performance of the cell with flow of methanol/water mix, with temperature and with current density was studied. Polarisation measurements indicate that the medium channel depth flow channels performed better than either the shallow depth or deep depth flow channels indicating that there is a complex relationship between the effect of flow velocity and the influence of the rate of production of product CO_2. AC impedance spectroscopy measurements confirmed the observed polarisation results. This method proved to be able to provide a reliable indication of the performance of the cell even when the cell had not yet achieved steady-state. In the case of the shallow channel depth anode, ac impedance revealed that it required considerably longer to achieve steady-state than the time required for the medium and deep channel depths.

Keywords: Fuel cells/direct methanol; Impedance spectroscopy (ac)

1. Introduction

Direct methanol fuel cells (DMFCs) have considerable advantages when compared to polymer electrolyte membrane (PEM) hydrogen/air fuel cells: simplicity and convenience. However, DMFCs are also marred by a number of technical challenges: very wet environment, slow anode kinetics and mixed potential [1–3].

The wet environment has important implications for the cell operation. An excess of water in DMFCs can lead to cathode flooding and, in consequence, results in less than optimal performance. The cell has to be designed in such a way as to keep water away from electrical connections. This is further complicated by the fact that corrosion restricts the choice of the material for channel plates.

A number of different approaches are being investigated to improve anode kinetics. The greatest effort is being directed toward the development of more active electrocatalysts: binary to quaternary platinum alloys [4], supported and unsupported Pt/Ru [5–8]. Other approaches for dealing with slow anode kinetics involve increased cell temperature and pressure [9].

A critical issue to the advancement of DMFC is methanol permeation through the membrane. Methanol is being ionised in the cathode catalyst layer, but the ions and electrons do not contribute to the overall current. Instead this consumes oxygen and, in consequence, lowers the overall voltage.

Until a methanol impermeable membrane is discovered [10–14] or the cathode catalyst possesses the specific function to selectively catalyse oxygen reduction without allowing methanol oxidation [15,16], the only known tools to reduce methanol crossover are lower methanol feed concentration and optimised cell design [17].

* Corresponding author. Tel.: +1-613-541-6000/ext. 6702; fax: +1-613-542-9849.
E-mail address: peppley-b@rmc.ca (B.A. Peppley).

0378-7753/01/$ – see front matter
PII: S0378-7753(01)00490-6

There has recently been a significant amount of work done in modelling the flow behaviour in DMFCs [18–23]. The performance of a variety of flow channel designs were also recently compared [24,25]. It is clear that the geometry of the flow channels (especially the anode channel) can have a significant effect on fuel cell performance.

Various approaches have been used in our laboratory to study the effect of anode flow characteristics on DMFC performance. The first experimental set-up used a transparent cell (Plexiglas™ and Cyrolon) with grid pattern flow channels. Current collectors, both mesh and foil, of various materials (graphite, stainless steal, titanium and molybdenum) were used in an attempt to achieve low contact resistance.

The transparent cell proved to be an excellent tool for gaining knowledge of the flow dynamics inside the DMFC. For example, it could be visually confirmed that the performance of the cell was significantly effected both by cathode flooding, and when the surface of the anode became covered with bubbles of carbon dioxide. This cell, however, had a somewhat limited operating temperature and pressure.

In the present work, a cell of standard filter-press configuration with parallel rectangular single-pass flow channel plates was used. Both the anode and cathode were made of electrochemical grade graphite. The variation of the performance of the cell was investigated with respect to flow velocity, temperature and concentration gradients in the boundary layer between the electrode and the flowing liquid, also for different depths of anode flow channels.

Anode and cathode characterisation by ac impedance was performed using a procedure similar to the one discussed in [26,27].

2. Experimental

The cell consisted of a membrane/electrode assembly sandwiched between two rectangular graphite plates which had been treated with zinc–phosphate resin to reduce gas permeation and fluid penetration (supplied by Poco Graphite Inc.). The active area of the cell was approximately 50 mm × 50 mm. Flow channels were machined into the graphite blocks. Three anode plates were fabricated with channel depths of 1.1905, 2.381 and 4.763 mm (shallow, medium and deep). The schematic representation of the flow channel configuration used in this study is shown in Fig. 1.

A single cathode plate was fabricated from graphite with a 1.1905 mm channel depth. The cathode was the mirror image of the shallow channel depth anode plate. The current collectors were made from molybdenum foil and placed to the back face of graphite plates. The cell was clamped between two GPO-3 fibreglass (glass polyester laminates) boards, two 6061-T6 aluminium plates and eight steel bolts to provide rigidity for the system and to distribute pressure equally across the plate surface/electrode interface. The methanol entered at the bottom and oxygen from the top. This orientation was chosen based on observation of

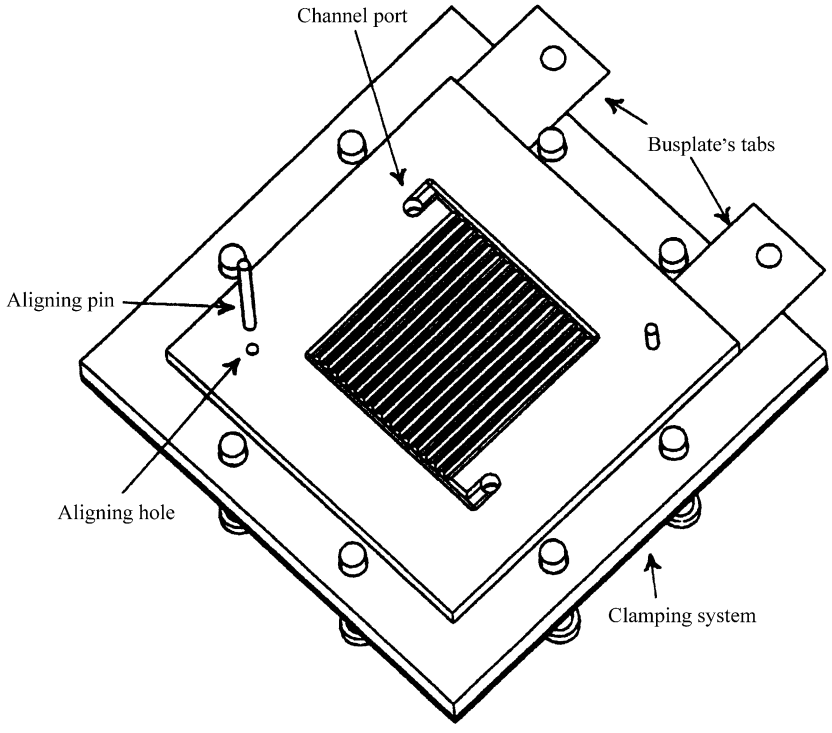

Fig. 1. Perspective view of the cell in its operational orientation. The top right aligning pin is shown inserted in the plate, as is the case during cell assembly.

the product CO_2 removal at the anode and liquid crossover at the cathode, within the transparent cell studied previously.

The membrane electrode assembly (MEA) used in the cell was purchased from E-TEK. It consisted of two electrodes containing the catalysts: anode (4 mg cm^{-2} (Pt–Ru)O_x (1:1 a/c)) and cathode (4 mg cm^{-2} Pt black) laminated to either side of a proton conducting solid polymer membrane (Nafion 117). The active surface area was 3025 mm^2. The space under the ridges between the channels was included in this value.

The cell was placed in the test rig, that consisted of a HPLC reciprocating piston pump (ISCO Model 2350) used to supply methanol solution from the reservoir, a programmable mass flow controller with digital signal processing from AALBORG to indicate and control oxygen flow rates (see Fig. 2). Methanol pressure was controlled by maintaining a back pressure of nitrogen in the collection vessel. This system, which was developed in-house, was able to compensate for fluctuations in the anode stream density caused by intermittent discharges of product CO_2. Ultra high purity oxygen was provided, at the required pressure, from a cylinder equipped with a two-stage stainless steel, low pressure, regulator. All the inlet connections between the cell and equipment were made of annealed 304 stainless steel ASTM A269 tubing. About 2.5 m of the tubing, in the form of a coil, was placed inside the oven in order to preheat the gas before being fed to the cell. Cole–Palmer pressure transmitters, range 0–6.9 bar (0–100 psi) ±0.25% of full scale, were mounted on the outlets of the streams. FEP fluoropolymer translucent tubing was used on all outlet connections to enable visual observations of the flow streams. The oven was equipped with a transparent door in order to monitor for methanol leaks.

The internal resistance of the cell was taken between the tabs of the anode current collectors and the tabs of the cathode current collector using a four terminal ac Hewlett-Packard milliohmeter (model 4328A).

A Labview data acquisition system was used to collect and store flow rates, pressures, temperature, voltage, current and internal resistance. Power and current densities were calculated and graphed continuously as voltage and applied load values were acquired. A bipolar operational power supply (BOP, 20–20 M) from Kepco was used to apply an appropriate load to the DMFC.

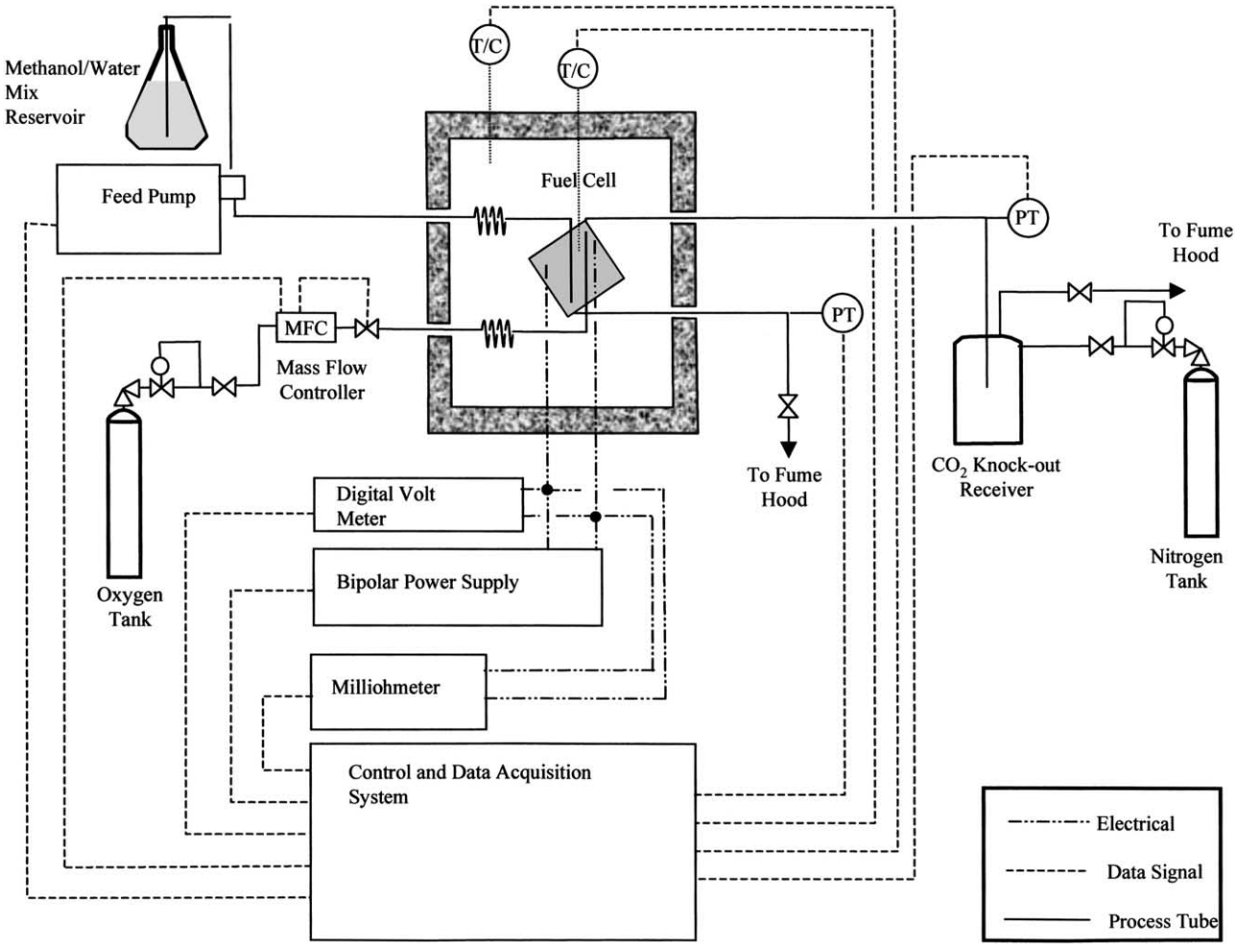

Fig. 2. Schematic of the test rig.

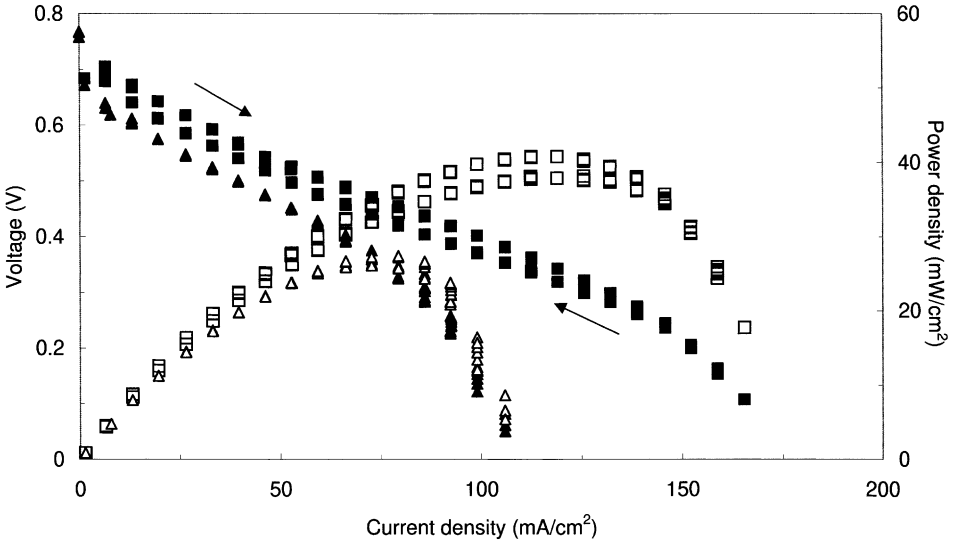

Fig. 3. Variation in fuel cell performance with temperature shown for medium channel depth. Methanol flow stoichiometric ratio = 4, O_2 flow = 0.25 SLM (kept constant throughout). (■) Voltage at 95°C; (□) power density at 95°C; (▲) voltage at 70°C; (△) power density at 70°C.

A Solartron (1255) hf frequency response analyser was used to perform ac impedance spectroscopy measurements. The BOP was adapted to work as a potentiostat in connection with the Solartron. A voltage divider (20:1) was placed between BOP and generator output from the Solartron.

Initial conditioning of the MEA was done in the cell. The anode was supplied with 1 M aqueous solution of methanol at 0.2 ml min^{-1}. The cathode was supplied with oxygen at 0.25 l min^{-1}. The cell was kept at 70°C for 48 h. No pressure was applied during conditioning.

To insure the same conditions for each experiment, the cell was conditioned for 2 h daily with an applied load corresponding to 40 mA cm^{-2} at pressure (50/50 psi, anode/cathode) and temperature (70 or 95°C).

If it is not stated otherwise, the methanol flows were adjusted relative to the current to maintain a four times stoichiometric ratio. Oxygen flow was kept constant at 0.25 SLM.

At each set of anode operating conditions, the cathode was supplied at first with oxygen and the polarisation and ac impedance were measured. The polarisation measurements were repeated after the ac impedance, to ensure that the fuel cell conditions were steady. Next nitrogen was fed to the cathode instead of oxygen. This is equivalent to having a

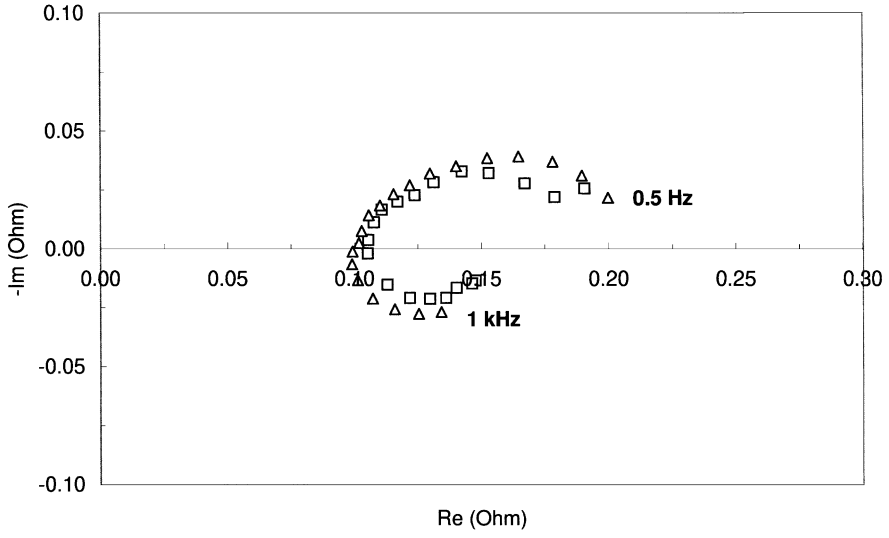

Fig. 4. Variation in ac impedance spectra with cell temperature. Channel depth = 2.4 mm, current density = 40 mA cm^{-2}, O_2 flow = 0.25 SLM. Methanol flow stoichiometric ratio = 4, ac amplitude = 5 mV. (□) 95°C; (△) 70°C.

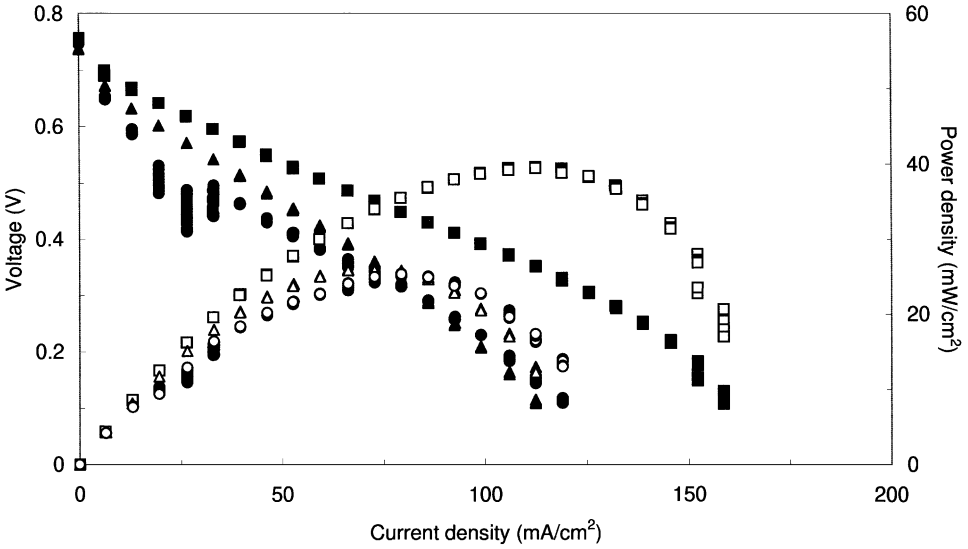

Fig. 5. Variation in fuel cell performance with channel depths. Other conditions as in Fig. 3. (●, ○) 1.2 mm; (□, ■) 2.4 mm; (▲, △) 4.8 mm. Solid symbols: voltage; outline symbols: power.

reference hydrogen electrode (RHE) since hydrogen is being generated at the cathode. The polarisation and ac impedance were measured after 1 h and repeated 18 h later.

For the polarisation curves, the applied current was increased by uniform intervals until the cell voltage reached 0.1 V. The current was then decreased in uniform intervals so that polarisation curves for increasing and decreasing loads were obtained.

AC impedance measurements were done at a base current density of 40 mA cm^{-2} (20 mA cm^{-2} for some measurements at 70°C) with the amplitude of the sinusoidal current signal adjusted so that potential amplitude was 5 mV. Impedance spectra were obtained at frequencies between 1 kHz and 0.5 Hz. The integration time was set at 10 s.

The data reported here were obtained with one MEA. All three anode channels were investigated with the medium channel depth (2.381 mm) repeated.

3. Results and discussion

3.1. Results from methanol/oxygen operation

Steady-state current–voltage characteristics of the cell were obtained at 70 and 95°C for all three channel depths. The polarisation and ac impedance results for medium channel depth at both temperatures are shown in Figs. 3 and 4, respectively. The flow rate of methanol was increased

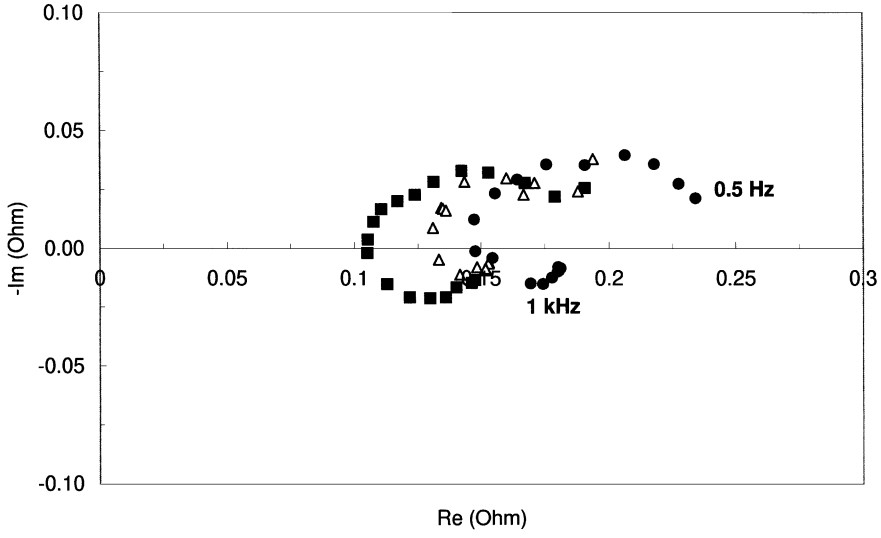

Fig. 6. An ac impedance spectra for (●) shallow; (■) medium; (△) deep channels at 95°C. Other conditions as in Fig. 4.

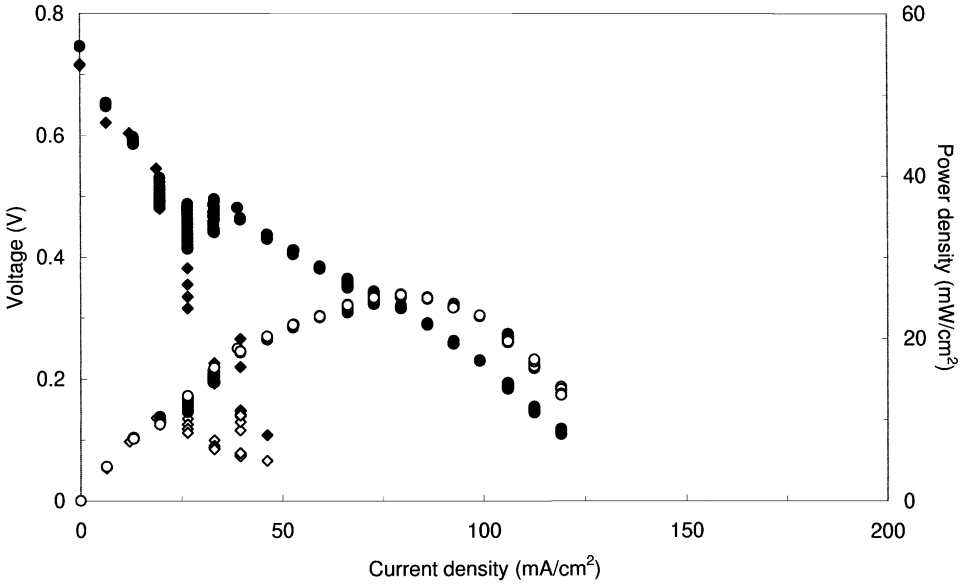

Fig. 7. Polarisation curves for shallow channel depth showing effect of slow response to load changes. Other conditions as in Fig. 3. (◆, ◇) Measurement 1; (●, ○) measurement 2. Solid symbols: voltage; outline symbols: power.

during polarisation measurements to maintain the stoichiometric ratio equal to four. A significantly lower power density and a lower maximum current density was obtained at 70 than at 95°C.

The ac impedance data for medium channel were obtained when the system was under a load corresponding to 40 mA cm^{-2} at 95 and at 70°C. Consistent with the polarisation data, Fig. 4 shows increased impedance at lower temperature in the high and low frequency regions.

Fig. 5 shows the variation in fuel cell performance with channel depth. From the three channel depths tested, the medium channel gave the best performance. The other channels (shallow and deep) gave similar values for power density, although the shallow one was more problematic to operate.

AC impedance spectra for the three channels depth at 95°C, current density of 40 mA cm^{-2} and methanol flow rate equivalent to a stoichiometric ratio of four, are shown in Fig. 6. As expected, the impedance in the real domain was greatest for the shallow channel depth flow plate.

Fig. 7 shows two polarisation curves obtained at 95°C for the shallow channel depth. Both measurements were done at a pressure of 350/350 kPa, anode/cathode and with anode feed rate increased with increasing load, to maintain a stoichiometric ratio of four. Fig. 8 shows the ac impedance spectra that were collected immediately following the

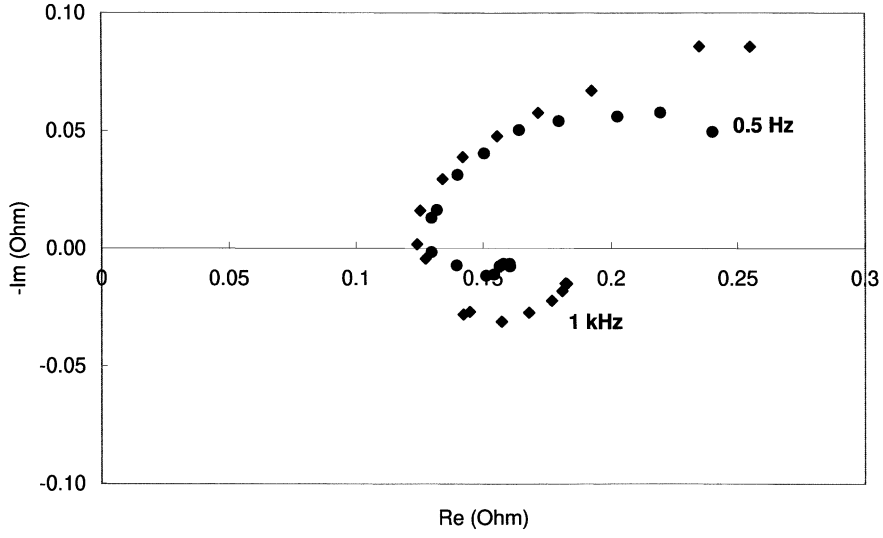

Fig. 8. An ac impedance spectra for shallow channel at 95°C. Current density = 20 mA cm^{-2}, O_2 flow = 0.25 SLM. Methanol flow stoichiometric ratio = 4. (◆) Measurement 1; (●) measurement 2. Performed after polarisation curves of Fig. 7.

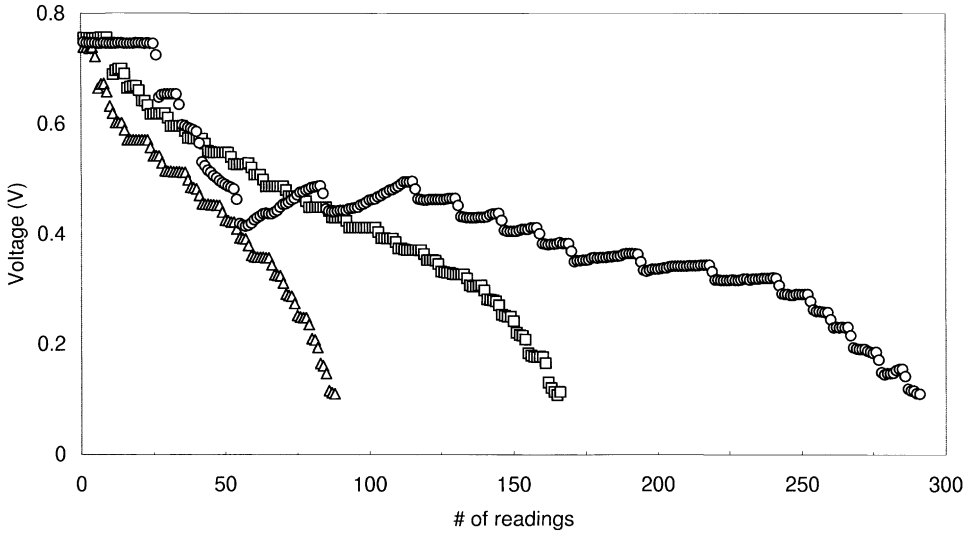

Fig. 9. Channel depth effect on achieving steady-state. Time between readings is 5 s. (△) 1.2 mm; (□) 2.4 mm; (○) 4.8 mm.

polarisation measurements in Fig. 7. As can be seen, the difference in the impedance spectra is not as significant as would be expected given the difference in polarisation curves. It was later determined, after reviewing the data collection files, that the first polarisation curve for the shallow channels had been collected from approximately 90 readings whereas the second polarisation curve had required nearly 300 readings. Clearly, the first polarisation curve did not represent steady-state performance. Fig. 9 shows this graphically. As can be seen, stable steady performance was achieved relatively quickly for the deep and medium depth flow channels; whereas, for the shallow flow channels there is a relatively slow recovery when the load is changed.

Additional investigations were completed to determine whether fuel cell performance with the shallow anode channels could be improved by increasing the flow velocity of the methanol solution. Figs. 10 and 11 shows that a stoichiometric ratio of four seems to be sufficient. Increasing the ratio to six did not significantly improve power density, but decreasing it to two lowered it drastically. In the lower current density range, between 10 and 50 mA cm^{-2}, the stoichiometric ratio of six appears to give slightly more stable performance than was observed for a stoichiometric ratio of four.

3.2. Results from reference hydrogen electrode

To separate the contribution of the oxygen reduction reaction to the overvoltage from the anode and membrane contributions, reference hydrogen electrode (RHE)

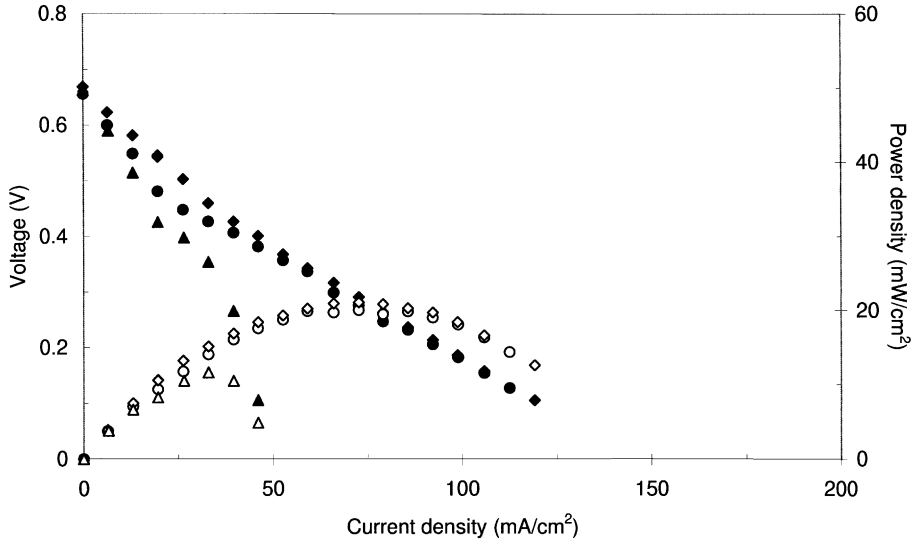

Fig. 10. Polarisation data for shallow channel at 95°C for methanol flow stoichiometric ratio of: (●) four; (◆) six; (▲) two. O_2 flow = 0.25 SLM. Solid symbols: voltage; outline symbols: power.

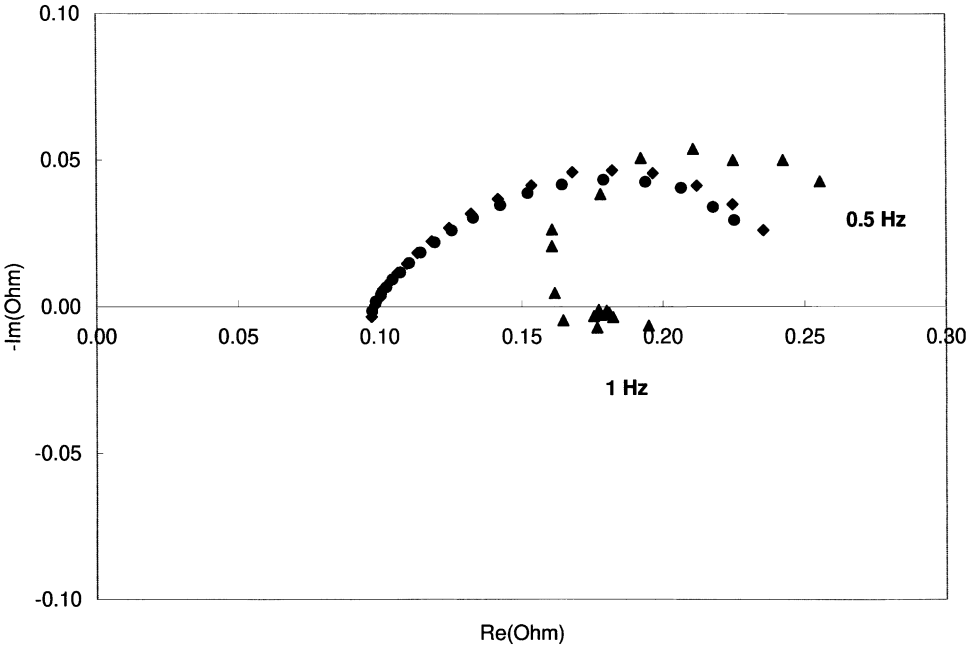

Fig. 11. AC impedance spectra for shallow channel at 95°C for methanol flow stoichiometric ratios of: (●) four; (◆) six; (▲) two.

measurements were taken. This was accomplished by feeding nitrogen to the cathode at a flow rate equal to that of the previous oxygen flow. Polarisation curves and impedance spectra were collected for this RHE configuration. By comparing these results with the methanol–oxygen performance measurements, an indication of the impact of the oxygen cathode performance on the cell can be separated from the anode–membrane effects.

Figs. 12 and 13 show the polarisation curve and the ac impedance spectrum taken when the cathode was supplied with nitrogen to give an equivalent to RHE configuration at 95°C for the medium depth channels. The oxygen–methanol polarisation curve and impedance spectrum are also shown for comparison. The methanol flow was four times stoichiometric for these measurements. As can be seen from Fig. 12, the cell voltage is negative for the RHE configuration. The open circuit voltage should be approximately −0.016 V according to the Nernst potential so that the overvoltage contribution of the oxygen electrode varies from 0.48 V at open circuit voltage to the 0.42 V at 160 mA cm^{-2}. By subtracting the cathode overvoltage from the total overvoltage, the overvoltage contribution of the anode–MEA

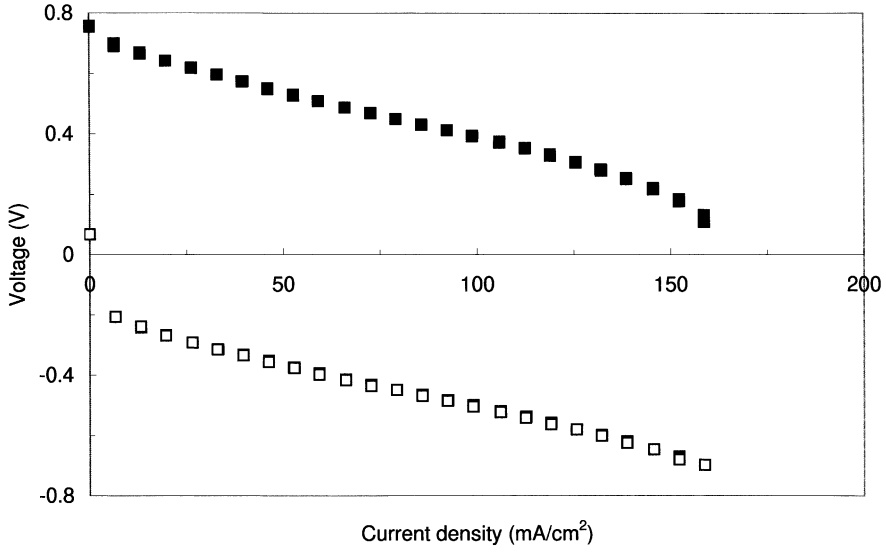

Fig. 12. The RHE–methanol and oxygen–methanol polarisation measurements for medium channel depth at 95°C. Other conditions as in Fig. 3. (■) Oxygen–methanol; (□) RHE–methanol.

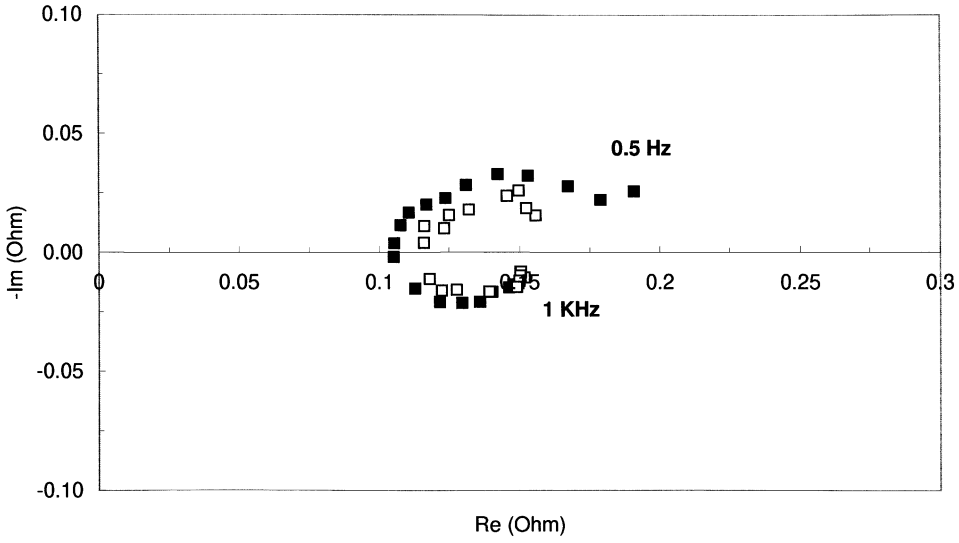

Fig. 13. The RHE–methanol and the oxygen–methanol ac impedance spectra for medium channel depth at 95°C. Other conditions as in Fig. 4. (■) Oxygen–methanol; (□) RHE–methanol.

was calculated to be zero at open circuit and 0.68 V at 160 mA cm^{-2} was calculated. By comparing this value with the total polarisation losses, we see that the anode–MEA accounts for approximately 60% of the voltage losses observed in the methanol–oxygen polarisation but there is clearly a contribution due to the oxygen electrode overpotential of 40% at 160 mA cm^{-2}. If we examine the ac impedance spectra, we see that the spectrum for the RHE measurements form an arc that is inside the methanol–oxygen spectrum. This confirms that the oxygen electrode makes a significant contribution to losses in the overall cell performance. The RHE polarisation measurements and ac impedance spectrum indicate that the overvoltage of the oxygen electrode accounts for more of the polarisation losses in the shallow (50% at 120 mA cm^{-2}) and deep (45% at 110 mA cm^{-2}) channel depths than in the medium channel depth configurations. It appears that the flow channel geometry has an effect on the rate of methanol crossover and consequently on the polarisation losses at the cathode, attributable to the parasitic oxidation of methanol. This effect on crossover may be associated with the masking of the anode by product CO_2 but more testing is required to confirm this hypothesis.

4. Conclusions

This is the first time that results from this test system have been published. The experimental apparatus performed well and has been able to generate accurate and reproducible results. The most significant control problem has been maintaining a uniform flow and pressure on the anode as the discharge of product CO_2 causes large changes in the density of the flowing fluid. The use of a pressurised receiving vessel to create a stable back pressure on the anode appears to have resolved this problem.

The effect of temperature on DMFC performance was as expected. The maximum power density at 95°C was approximately 50% greater than at 70°C. The performance at the higher temperature in general was more stable.

The initial study of the effect of flow channel depth has revealed that there is a complex relationship between flow geometry and DMFC performance. The medium channel depth anode flow field consistently showed the best performance. The polarisation losses for the shallow channel depth and the deep channel depth anodes were similar and were significantly and consistently less than the medium channel depth anode. A key characteristic of the shallow channel depth performance was that it took a much greater amount of time to reach steady-state than for the other two channel configurations. This may be due to the larger pressure drop through the anode and time required to achieve a stable pressure gradient following a change in methanol flow. An ac impedance spectroscopy gave an indication that there was an initial polarisation data for the shallow depth channels.

Comparing the RHE measurements with the oxygen–methanol data provides an indication of the relative importance of the cathode polarisation to the performance of the DMFC. From this analysis it has been determined that the contribution of the cathode to the fuel cell overvoltage is less than the anode–membrane contribution but is still quite significant.

Acknowledgements

Support for this work was provided by the Canadian Department of National Defence through the Defence Research and Development Branch.

References

[1] M. Baldauf, W. Preidel, J. Power Sources 84 (1999) 161.
[2] A. Heinzel, V.M. Barragan, J. Power Sources 84 (1999) 70.
[3] S. Wasmus, A. Küver, J. Electroanal. Chem. 461 (1999) 14.
[4] B. Gurau, R. Viswanathan, R. Liu, T.J. Lafrenz, K.L. Ley, E.S. Smotkin, E. Reddington, A. Sapienza, B.C. Chan, T.E. Mallouk, S. Sarangapani, J. Phys. Chem. B 102 (1998) 9997.
[5] D.R. Rolison, P.L. Hagans, K.E. Swider, J.W. Long, Langmuir 15 (1999) 774.
[6] K.A. Friedrich, M. Huber, M. Stefener, U. Stimming, Fuel Cell Seminar Abstracts, Portland, USA, 2000, p. 190.
[7] A.S. Arico, V. Baglio, P. Creti, V. Antonucci, Fuel Cell Seminar Abstracts, Portland, USA, 2000, p. 75.
[8] L. Liu, C. Pu, R. Viswanathan, Q. Fan, R. Liu, E.S. Smotkin, Electrochem. Acta 43 (1998) 3657.
[9] A.S. Arico, P. Creti, P.L. Antonucci, J. Cho, H. Kim, V. Antonucci, Electrochem. Acta 43 (1998) 3719.
[10] P. Staiti, M. Minutoli, S. Hocevar, J. Power Sources 90 (2000) 231.
[11] C. Pu, W. Huang, K.L. Ley, E.S. Smotkin, J. Electrochem. Soc. 142 (1995) L119–120.
[12] B.S. Pivovar, Y. Wang, E.L. Cussler, J. Membr. Sci. 154 (1999) 155.
[13] E. Peled, T. Duuvdevani, A. Melman, Electrochem. Solid State Lett. 1 (1998) 210.
[14] N. Yoshida, T. Ishisaki, A. Watakabe, M. Yoshitake, Electrochem. Acta 43 (1998) 3749.
[15] D. Chu, R. Jiang, Ch. Walker, Fuel Cell Seminar Abstracts, Portland, USA, p. 160.
[16] R.W. Reeve, P.A. Christensen, A. Hamnett, S.A. Haydock, S.C. Roy, J. Electrochem. Soc. 145 (1998) 3463.
[17] X. Ren, P. Zelenay, S. Thomas, J. Davey, S. Gottesfeld, J. Power Sources 86 (2000) 111.
[18] K. Scott, W. Taama, J. Cruickshank, J. Appl. Electrochem. 28 (1998) 289.
[19] D. Xue, Z. Dong, J. Power Sources 76 (1998) 69.
[20] S.F. Baxter, V.S. Battaglia, R.E. White, J. Electrochem. Soc. 146 (1999) 437.
[21] P. Argyropoulos, K. Scott, W.M. Taama, J. Appl. Electrochem. 30 (2000) 899.
[22] A.A. Kulikovsky, J. Appl. Electrochem. 30 (2000) 1005.
[23] H. Dohle, J. Divisek, R. Jung, J. Power Sources 86 (2000) 469.
[24] K. Scott, P. Argyropoulos, C. Jackson, W.M. Taama, J. Horsfall, K. Lovell, K. Soundmacher, Fuel Cell Seminar Abstracts, Portland, USA, 2000, p. 110.
[25] H. Dohle, T. Bewer, J. Merger, R. Neitzel, D. Stolten, Fuel Cell Seminar Abstracts, Portland, USA, 2000, p. 130.
[26] J.T. Mueller, P.M. Urban, J. Power Sources 75 (1998) 139.
[27] J.T. Müller, P.M. Urban, W.F. Hölderich, J. Power Sources 84 (1999) 157.